Published in final edited form as:
Langmuir. 2012 June 12; 28(23): 8589–8593. doi:10.1021/la300268d.

Controlling the Surface Chemistry of Graphite by Engineered Self-Assembled Peptides

Dmitriy Khatayevich, **Christopher R. So**, **Yuhei Hayamizu**, **Carolyn Gresswell**, and **Mehmet Sarikaya***
Materials Science and Engineering; Genetically Engineered Materials Science and Engineering Center, University of Washington 302 Roberts Hall, Seattle, WA 98195 (USA)

Abstract

The systematic control over surface chemistry is a long-standing challenge in biomedical and nanotechnological applications for graphitic materials. As a novel approach, we utilize graphite-binding dodecapeptides that self-assemble into dense domains to form monolayer thick long-range ordered films on graphite. Specifically, the peptides are rationally designed through their amino acid sequences to predictably display hydrophilic and hydrophobic characteristics while maintaining their self-assembly capabilities on the solid substrate. The peptides are observed to maintain a high tolerance for sequence modification, allowing the control over surface chemistry *via* their amino acid sequence. Furthermore, through a single step co-assembly of two different designed peptides, we predictably and precisely tune the wettability of the resulting functionalized graphite surfaces from 44 to 83 degrees. The modular molecular structures and predictable behavior of short peptides demonstrated here give rise to a novel platform for functionalizing graphitic materials that offers numerous advantages, including non-invasive modification of the substrate, bio-compatible processing in an aqueous environment, and simple fusion with other functional biological molecules.

Controlling interfacial properties of materials through surface functionalization of solid substrates has been a major challenge in medicine and nanotechnology for the last two decades.[1,2] The precise display of function and chemistry is particularly critical for engineering bio-inorganic interfaces, where the orientation and density of the immobilized molecules may have direct bearing on the performance of the resulting assembly, such as, for example, the specific activity of immobilized enzymes.[3] Biocombinatorially selected (through phage or cell-surface display) and genetically engineered solid-binding peptides offer a versatile platform for bridging the bio/inorganic divide.[4–7] These strong-binding (k_d ~ 50 nM to 1 μM), material-specific 7–14 amino acid long sequences possess a wealth of chemical diversity and modular capacity through mutation and targeted chemical modification, providing unique opportunities for tuning binding, chemical properties and display.[8,9] Rather than covalent bonding, prevalent in synthetic linkers, such as silanes, thiols, and phosphanates,[10,11] short peptides bind through weak forces at multiple positions at the peptide/solid interface with the advantage of assembling and functioning in aqueous solutions.[12,13] As biocompatible coatings, therefore, solid-binding peptides are particularly well suited for applications in medical and biological fields because they are produced and

sarikaya@u.washington.edu.

SUPPORTING INFORMATION AVAILABLE:
Supporting information includes: detailed experimental procedures, mass spectra of peptides, application and discussion of Cassie's Law, amorphous versus ordered phase roughness comparison, liquid surface tension data, and verification of ss-GrBP5 assembly by AFM. This material is available free of charge via the Internet at http://pubs.acs.org.

function under biological conditions, and have not shown any toxicity in cell culture studies.[7,14,15]

Graphite, graphene and carbon nano-tubes (CNT) have been employed for both biomedical and nanotechnological applications due to their anti-microbial activity,[16] high conductivity, optical transparency, and surface sensitive properties.[17–20] These graphitic materials have been employed for biosensing applications in particular due to their excellent electronic properties, resulting from delocalized π bonds on the surface.[21–23] A number of functionalization routes through covalent bonding, i.e. the introduction of carboxylic groups, have been employed to control the interface with graphitic materials.[24,25] In parallel, however, to preserve the intrinsic properties of these materials, methods of non-covalent functionalization via π−π stacking using aromatic chemistry have been used to assemble functional molecules.[26,27] In addition to these successful chemical functionalization techniques, a non-invasive approach using peptides could present a biocompatible alternative to controlling the surface properties of graphite. Here, we demonstrate precise control over the hydropathy of graphite through single-step self-assembly of peptides and their engineered mutants. The graphite binding peptides are modular and can be designed to self-assemble into stable monomolecular films on graphite, exposing predictable surface chemistry through the display of specific amino acids. The highly oriented pyrolytic graphite (HOPG) has an atomically flat surface which is ideally suited to demonstrate, using atomic force microscopy and contact angle measurements, the display of tailored chemistries on graphite through controlling the binding and assembly of the designed peptides, in the absence of roughness effects.[28]

Various graphite-[29], graphene-,[30–32] and CNT-binding[33,34] peptide sequences and poly amino acids have been identified in literature. They have been employed for applications such as bioinorganic nano-structure formation[35] as well as non-specific control of surface chemistry[29].

The dodecapeptide used in this work, GrBP5-WT (Sequence: IMVTESSDYSSY, affinity constant: K_a=3.78μM^{-1})[36] is unique among graphite- and CNT-binding peptide sequences identified so far, as it forms long-range ordered, uniform, and crystallographic molecular nanostructures on HOPG (Figure 1a), which can be controlled through sequence mutation. The abbreviation WT denotes the original, unmodified, sequence of the peptide, which we call “wild type”. In previous work,[36] it was found that the self-assembly of GrBP5-WT arises from a combination of binding through the aromatic rings of tyrosine residues at the C-terminus, and ordering through intermolecular interactions among hydrophobic tail domains (Figure 1b). The formation of ordered morphology, apparent from Figure 1a, and evidenced by the FFT, seems to be a result of both lattice matching with the underlying HOPG, which results in six-fold symmetry, and assembly conditions, such as concentration, which, along with intermolecular interactions, determines the size of features.[36] Replacing the hydrophobic residues at the N-terminus with hydrophilic ones, therefore, inhibits formation of the ordered phase (OP) and causes the peptide film to remain in the amorphous phase (AP) because of the lack of intermolecular interactions (Figure 1c and d). Furthermore, it was found that an ordered film of GrBP5-WT displays hydrophobic property on the graphite surface (Figure 1a). These findings motivated us to hypothesize that ordered structures of GrBP5-WT leave the N-terminus aminoacids free for rational control of intermolecular interactions as well as further functionalization, and predictable display of specific chemistry. Based on this hypothesis, we aim here to demonstrate that the wettability of graphite can be controlled by varying the N-terminal sequence of the GrBP5-WT peptide. Specifically, we design two mutants (i.e., variants of the WT peptide) which exhibit hydrophobic or hydrophilic properties while retaining their ordered structure and predictable display capability. The hydrophobic mutant GrBP5-Phob is produced by substitution of the

three N-terminal amino-acids of the wild type with a more hydrophobic LIA sequence (Table 1). The hydrophilic hybrid mutant SS-GrBP5 (Figure 1e, Table 1), on the other hand, is designed by the addition of two hydrophilic serine residues to the N-terminus of the wild type peptide.

To characterize the wettability of the peptide-functionalized graphite surfaces, freshly prepared HOPG substrates were incubated in 1μM aqueous peptide solutions (Table 1) for several time intervals, resulting in samples of peptide films on the graphite surface that range from sparse to near-confluent monolayers. The wettability of these films was quantified by contact angle goniometry, and the coverage was determined by atomic force microscopy (AFM) (See supporting information for detailed procedures). The plot of coverage *vs.* contact angle values exhibits a coinciding linear correlation below 70% coverage for all peptides (Figure 2a, red). Above 70%, they also display linear relationships but with slopes that vary greatly with sequence (Figure 2a, blue).

To quantitatively compare the wettability of different peptides, we applied Cassie's Law,[37] which describes the contact angle, cos θ, of a macroscopic droplet on a chemically heterogeneous surface *via* the relation: $\cos\theta = \varphi_g \cos\theta_g + \varphi_p \cos\theta_p$ ($\varphi_{g,p}$: coverage and $\theta_{g,p}$: contact angle for graphite and peptides, respectively). By fitting this equation to the experimental data, effective contact angles are extrapolated for fully covered surfaces of each peptide, θ_p, (Table 2, also see supporting information for further discussion). Between 0 and 70% coverage, all peptides display little difference in θ_p (about 28°±4°). The θ_p values above 70% coverage of GrBP5-WT and GrBP5-Phob, however, are drastically different.

These results are also reflected in the corresponding AFM experiments (Figure 2b) where peptides are observed to form one of the two phases on the surface: either a long-range ordered phase (OP) at high coverage, exhibiting six-fold symmetry, or a sparse amorphous phase (AP) at low coverage without recognizable crystallographic symmetry in the formed film. There is an effective transition threshold from AP to OP at about 70% coverage. Ordered peptide films also exhibit more uniform and narrow distributions of thickness as measured by AFM, which is apparent from the average roughness values in Table 2, (Figure S2). Only GrBP5-Phil, with no hydrophobic tail, remained disordered under all incubation conditions.

The similarity in the θ_p contact angles of all peptides in the AP below 70% coverage may indicate that the exposed amino acid domain is conserved among mutants and is predominantly hydrophilic. This is most likely due to the random alignment of peptides displaying polar residue- and a serine-rich domain in the central portion of the peptide (Table 1). Conversely, the contrast between the contact angle contribution of GrBP5-WT (64.0°) and GrBP5-Phob (87.0°) in the OP implies that the three amino-acids at the N-terminus are uniformly exposed towards the solution, since they are the only ones that differ between the two peptide sequences.

Remarkably, both the binding and ordering capabilities of the peptides were retained in the SS-GrBP5 mutant (Figure 2, S3). Even in the ordered state, the SS-GrBP5 mutant has a contact angle contribution close to that of the AP (Table 2), indicating that hydrophilic residues are displayed in both of its phases of the peptide films. The difference in the contribution of the two phases, about 9°, confirms a transition from AP to OP, seen clearly in Figure 2, on surfaces functionalized by SS-GrBP5.

The uniform display of N-terminal residues by self-assembling peptides forming confluent ordered films on graphite results in a wide range of wettability values. It is, therefore, plausible to further tune the contact angle through a simultaneous high coverage, single-step,

co-assembly of peptides with varying wettability. We chose the two mutants that retained their assembly capabilities and exhibited the widest range of θ_p, i.e., 36.0° and 87.0°, to achieve precise control over the wettability of graphite surfaces at a constant coverage. For this, 1μM aqueous solutions of GrBP5-Phob and the SS-GrBP5 were mixed in appropriate proportions and incubated on HOPG for 3 hours, assuming the complete solubility of the two peptides solutions. The AFM images and contact angle versus fraction coverage dependencies are shown in Figure 3. While the peptide coverage of these films remained at around 80%, the contact angles of functionalized surfaces varied from 44.0° to 83.0°. The linear nature of the plot and the uniformity of the AFM images indicate that GrBP5-Phob is homogeneously dispersed within the film formed by SS-GrBP5. Moreover, by adding a third term to Cassie's equation, we were able to predict the cosine of the contact angle resulting from a given mixed monolayer based on the θp values from Table 2 (Figure 3). The agreement between the prediction and the data is quite close (Coefficient of determination, based on sum of squares of error is $R^2 = 0.96$). The small discrepancy in the predicted and measured values could result from a slight variation in the binding affinities of the two peptides, whereby SS-GrBP5 is present on the surface in slightly higher proportion than the GrBP5-Phob under the same incubation conditions.

Controlling surface wettability through self-assembled peptides provides a novel approach for engineering biomolecule/graphite interfaces. Mixed self-assembled peptide films prepared in water could lead to the development of bio-sensors with optimized chemical properties and biocompatibility. If better understood, the intermolecular interactions among different peptides in the ordered phase could be tailored to form novel, complex nanostructures with spatially controlled structural and biofunctional properties. Furthermore, the ease with which displayed amino acid domains are introduced into short peptides provides an opportunity to develop biomolecular constructs with designer proteins,[38,39] peptide domains,[13,40] and chemical groups[5,7] to further control functionality of graphitic surfaces. This inherently biocompatible and non-covalent molecular immobilization approach is suitable for a variety of potential applications of graphite, and graphitic materials, in nanobiotechnology.

Supplementary Material

Refer to Web version on PubMed Central for supplementary material.

Acknowledgments

The major funding (DK, CRS, CG, MS) for this research was supported by NSF-Biomaterials (DMR-0706655) and MRSEC programs (DMR-0520567) at GEMSEC, Genetically Engineered Materials Science and Engineering Center, University of Washington and NSF Biomaterial Program. DK and CRS were supported by the NCI Training Grant T32CA138312. YH was supported by JST PRESTO programs (Japan). The work was carried out at GEMSEC-SECF, a member of Materials Facilities Network of MRSEC. The content is solely the responsibility of the authors and does not necessarily represent the official views of the National Cancer Institute or the National Institutes of Health.

References

1. Chen D, Wang G, Li JH. Interfacial bioelectrochemistry: Fabrication, properties and applications of functional nanostructured biointerfaces. J Phys Chem C. 2007; 111:2351–2367.
2. Nel AE, Madler L, Velegol D, Xia T, Hoek EMV, Somasundaran P, Klaessig F, Castranova V, Thompson M. Understanding Biophysicochemical Interactions at the Nano-bio Interface. Nat Mater. 2009; 8:543–557. [PubMed: 19525947]
3. Cha T, Guo A, Zhu XY. Enzymatic Activity on a Chip: The Critical Role of Protein Orientation. Proteomics. 2005; 5:416–419. [PubMed: 15627963]

4. Tamerler C, Khatayevich D, Gungormus M, Kacar T, Oren EE, Hnilova M, Sarikaya M. Molecular Biomimetics: GEPI-Based Biological Routes to Technology. Biopolymers. 2010; 94:78–94. [PubMed: 20091881]
5. Shiba K. Exploitation of Peptide Motif Sequences and their Use in Nanobiotechnology. Curr Opin in Biotechnol. 2010; 21:412–425.
6. Peelle BR, Krauland EM, Wittrup KD, Belcher AM. Design Criteria for Engineering Inorganic Material-Specific Peptides. Langmuir. 2005; 21:6929–6933. [PubMed: 16008405]
7. Meyers SR, Khoo XJ, Huang X, Walsh EB, Grinstaff MW, Kenan DJ. The Development of Peptide-Based Interfacial Biomaterials for Generating Biological Functionality on the Surface of Bioinert Materials. Biomaterials. 2009; 30:277–286. [PubMed: 18929406]
8. Sarikaya M, Tamerler C, Jen AKY, Schulten K, Baneyx F. Molecular Biomimetics: Nanotechnology Through Biology. Nat Mater. 2003; 2:577–585. [PubMed: 12951599]
9. Wei JH, Kacar T, Tamerler C, Sarikaya M, Ginger DS. Nanopatterning Peptides as Bifunctional Inks for Templated Assembly. Small. 2009; 5:689–693. [PubMed: 19267336]
10. Ulman A. Formation and Structure of Self-Assembled Monolayers. Chem Rev. 1996; 96:1533–1554. [PubMed: 11848802]
11. Gawalt ES, Avaltroni MJ, Koch N, Schwartz J. Self-Assembly and Bonding of Alkanephosphonic Acids on the Native Oxide Surface of Titanium. Langmuir. 2001; 17:5736–5738.
12. Hnilova M, Oren OO, Seker UOS, Wilson BR, Collino S, Evans JS, Tamerler C, Sarikaya M. Effect of Molecular Conformations on the Adsorption Behavior of Gold-Binding Peptides. Langmuir. 2008; 24:12440–12445. [PubMed: 18839975]
13. Tamerler C, Sarikaya M. Molecular Biomimetics: Nanotechnology and Bionanotechnology Using Genetically Engineered Peptides. Phil Trans R S A. 2009; 367:1705–1726.
14. Khatayevich D, Gungormus M, Yazici H, So C, Cetinel S, Ma H, Jen A, Tamerler C, Sarikaya M. Biofunctionalization of Materials for Implants Using Engineered Peptides. Acta Biomater. 2010; 6:4634–4641. [PubMed: 20601249]
15. Yuca E, Karatas AY, Seker UOS, Gungormus M, Dinler-Doganay G, Sarikaya M, Tamerler C. In Vitro Labeling of Hydroxyapatite Minerals by an Engineered Protein. Biotechnol Bioeng. 2011; 108:1021–1030. [PubMed: 21190171]
16. Hu WB, Peng C, Luo WJ, Lv M, Li XM, Li D, Huang Q, Fan CH. Graphene-Based Antibacterial Paper. ACS Nano. 2010; 4:4317–4323. [PubMed: 20593851]
17. Balandin AA, Ghosh S, Bao WZ, Calizo I, Teweldebrhan D, Miao F, Lau CN. Superior Thermal Conductivity of Single-Layer Graphene. Nano Lett. 2008; 8:902–907. [PubMed: 18284217]
18. Castro Neto AH, Guinea F, Peres NMR, Novoselov KS, Geim AK. The Electronic Properties of Graphene. Rev Mod Phys3. 2009; 81:109–162.
19. Dai HJ. Carbon Nanotubes:3 Synthesis, Integration, and Properties. Acc Chem Res. 2002; 35:1035–1044. [PubMed: 12484791]
20. Novoselov KS, Geim AK, Morozov SV, Jiang D, Zhang Y, Dubonos SV, Grigorieva IV, Firsov AA. Electric Field Effect in Atomically Thin Carbon Films. Science. 2004; 306:666–669. [PubMed: 15499015]
21. Gorton, L. Biosensors and modern biospecific analytical techniques. Elsevier Science; Amsterdam, Netherlands: 2005.
22. Du D, Zou ZX, Shin YS, Wang J, Wu H, Engelhard MH, Liu J, Aksay IA, Lin YH. Sensitive Immunosensor for Cancer Biomarker Based on Dual Signal Amplification Strategy of Graphene Sheets and Multienzyme Functionalized Carbon Nanospheres. Anal Chem. 2010; 82:2989–2995. [PubMed: 20201502]
23. Lin YH, Lu F, Tu Y, Ren ZF. Glucose Biosensors Based on Carbon Nanotube Nanoelectrode Ensembles. Nano Lett. 2004; 4:191–195.
24. Li D, Muller MB, Gilje S, Kaner RB, Wallace GG. Processable Aqueous Dispersions of Graphene Nanosheets. Nat Nanotechnol. 2008; 3:101–105. [PubMed: 18654470]
25. Niyogi S, Bekyarova E, Itkis ME, McWilliams JL, Hamon MA, Haddon RC. Solution Properties of Graphite and Graphene. J Am Chem Soc. 2006; 128:7720–7721. [PubMed: 16771469]

26. Choi EY, Han TH, Hong JH, Kim JE, Lee SH, Kim HW, Kim SO. Noncovalent Functionalization of Graphene with End-Functional Polymers. J Mater Chem. 2010; 20:1907–1912.
27. Ghosh A, Rao KV, Voggu R, George SJ. Non-Covalent Functionalization, Solubilization of Graphene and Single-Walled Carbon Nanotubes with Aromatic Donor and Acceptor Molecules. Chem Phys Lett. 2010; 488:198–201.
28. Yu X, Wang ZQ, Jiang YG, Zhang X. Surface Gradient Material: From Superhydrophobicity to Superhydrophilicity. Langmuir. 2006; 22:4483–4486. [PubMed: 16649753]
29. Yang H, Fung S, Sun W, Mikkelsen S, Pritzker M, Chen P. Ionic-Complementary Peptide-Modified Highly Ordered Pyrolytic Graphite Electrode for Biosensor Application. Biotenol Prog. 2008; 24:964–971.
30. Cui Y, Kim SN, Jones SE, Wissler LL, Naik RR, McAlpine MC. Chemical Functionalization of Graphene Enabled by Phage Displayed Peptides. Nano Lett. 2010; 10:4559–4565. [PubMed: 20942387]
31. Wang QH, Hersam MC. Room-Temperature Molecular-Resolution Characterization of Self-Assembled Organic Monolayers on Epitaxial Graphene. Nat Chem. 2009; 1:206–211. [PubMed: 21378849]
32. Kim SN, Kuang Z, Slocik JM, Jones SE, Cui Y, Farmer BL, McAlpine MC, Naik RR. Preferential Binding of Peptides to Graphene Edges and Planes. J Am Chem Soc. 2011; 133:14480–14483. [PubMed: 21861527]
33. Kase D, Kulp JL, Yudasaka M, Evans JS, Iijima S, Shiba K. Affinity Selection of Peptide Phage Libraries Against Single-Wall Carbon Nanohorns Identifies a Peptide Aptamer with Conformational Variability. Langmuir. 2004; 20:8939–8941. [PubMed: 15379530]
34. Tomasio SM, Walsh TR. Modeling the Binding Affinity of Peptides for Graphitic Surfaces. Influences of Aromatic Content and Interfacial Shape. J Phys Chem C. 2009; 113:8778–8785.
35. Han TH, Lee WJ, Lee DH, Kim JE, Choi E, Kim SO. Peptide/Graphene Hybrid Assembly into Core/Shell Nanowires. Adv Mater. 2010; 22:2060–2064. [PubMed: 20352629]
36. So CR, Hayamizu Y, Yazici H, Gresswell C, Khatayevich D, Tamerler C, Sarikaya M. Controlling Self-Assembly of Engineered Peptides on Graphite by Rational Mutation. ACS Nano. 2012; 6:1648–1656. [PubMed: 22233341]
37. Cassie ABD, Baxter S. Wettability of Porous Surfaces. Trans Faraday Soc. 1944; 40:0546–0550.
38. Kacar T, Zin MT, So CR, Wilson BR, Ma H, Gul-Karaguler N, Jen AK-Y, Sarikaya M, Tamerler C. Directed Self-Immobilization of Alkaline Phosphatase on Micro-Patterned Substrates Via Genetically Fused Metal-Binding Peptide. Biotechnol Bioeng. 2009; 103:696–705. [PubMed: 19309754]
39. Hall Sedlak R, Hnilova M, Gachelet E, Przybyla1 L, Dranow D, Gonen T, Sarikaya M, Tamerler C, Traxler B. An Engineered DNA-Binding Protein Self-assembles Metallic Nanostructures. Chembiochem. 2010; 11:2108–2112. [PubMed: 20827792]
40. Hnilova M, Khatayevich D, Carlson A, Oren EE, Gresswell C, Zheng S, Ohuchi F, Sarikaya M, Tamerler C. Single-Step Fabrication of Patterned Gold Film Array by an Engineered Multi-Functional Peptide. J Colloid Interface Sci. 2012; 365:97–102. [PubMed: 21962430]

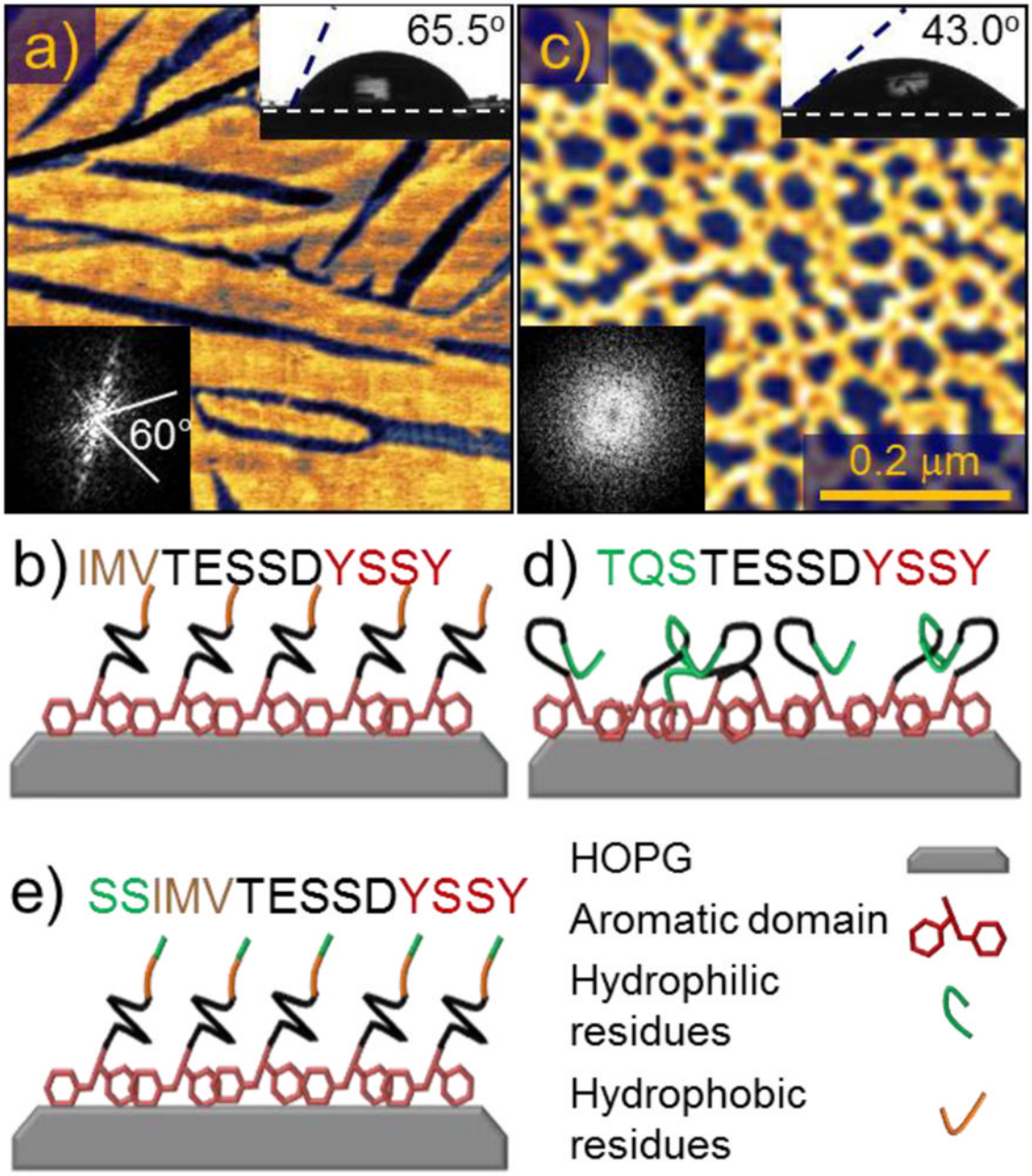

Figure 1.

(a) Atomic force microscopy (AFM) image of the peptide GrBP5-WT on graphite with (b) Corresponding sequence (N- to C-terminus) and its schematics. (c) AFM image of GrBP5-Phil mutant on graphite with (d) Corresponding sequence and its schematics. Insets show the contact angles and the Fast Fourier Transforms (FFT) of the images that highlights the presence (spots or lines) or the lack of ordering (featureless). Schematics in (b), (d) and (e) illustrate the hypothetical conformation of the peptides within the film which produce the observed contact angles, binding through the aromatic region, and displaying either the ordered hydrophobic or disordered hydrophilic residues.

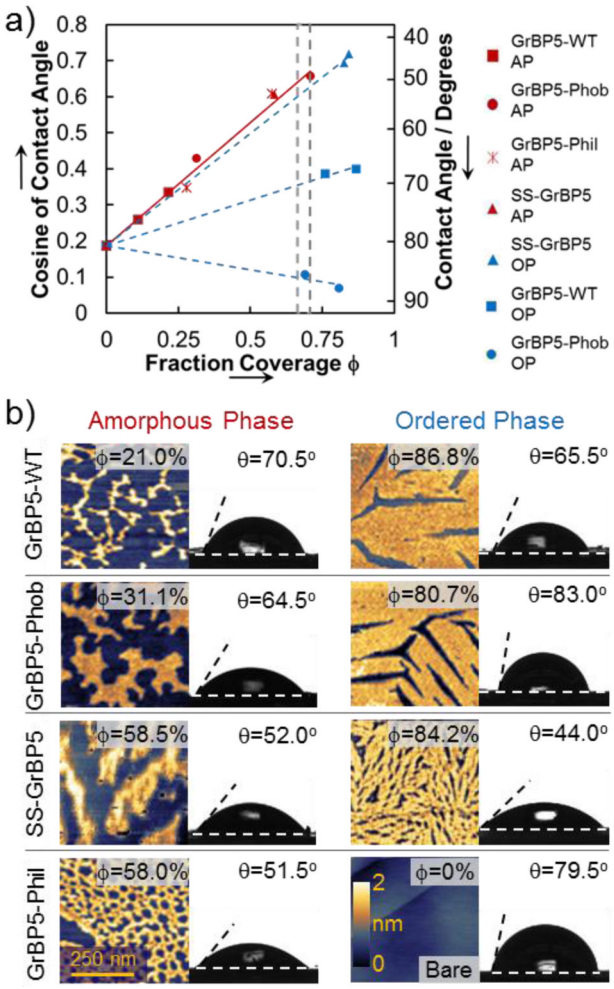

Figure 2.

(a) Plot of contact angle θ versus fraction coverage φ of peptides on graphite. The blue lines indicate linear trends above 70% coverage; the red line represents the linear trend for all peptides below 70% coverage. The change in slope between ordered (OP) and amorphous (AP) trend lines indicates the change in the displayed chemistry. The grey lines indicate the AP to OP transition region (b) AFM images showing typical examples of AP and OP structures, as well as the corresponding coverage and contact angles.

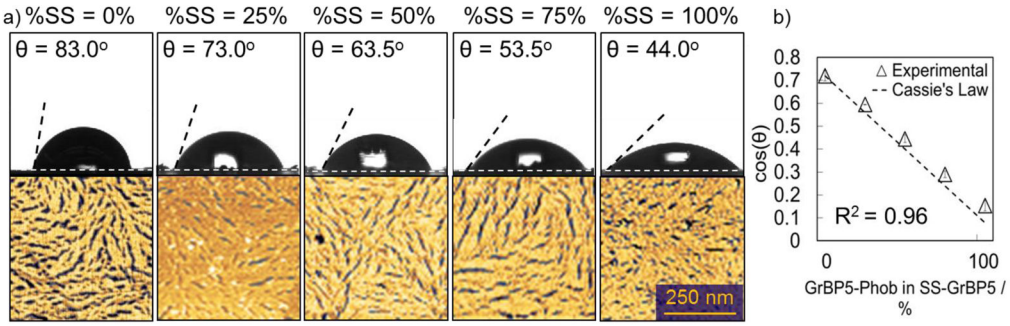

Figure 3.

(a) Contact angles and AFM images of ordered co-assembled peptide monolayer containing SS-GrBP5 and GrBP5-Phob. Coverage for all surfaces is greater than 80%. (b) Plot of cosine of the contact angle versus % of GrBP5-Phob mixed in SS-GrBP5 shows agreement with the trend predicted by Cassie's Law.

Table 1

Peptide sequences, weights, and hydropathy indices

Peptide	Sequence	Mol. Mass	G.R.A.V.Y.[a]
GrBP5-WT	IMV-TESSDYSSY	1381.4	−0.242
GrBP5-Phob	LIA-TESSDYSSY	1335.3	−0.283
GrBP5-Phil	TQS-TESSDYSSY	1354.3	−1.542
SS-GrBP5	SSIMV-TESSDYSSY	1555.6	−0.321

[a]Grand average hydropathy index

Table 2

Projected contact angles of a theoretical 100% peptide-covered sample for each peptide and phase, and corresponding measured roughness values.

Peptide	θ_p AP (0–70% coverage)	AP Roug./nm	θ_p OP (>70% coverage)	OP Rough./nm
GrBP5-WT	30.0°±2.5°	0.92	64.0°±1.0°	0.39
GrBP5-Phob	23.0°±11.5°	0.53	87.0±0.5°	0.36
GrBP5-Phil	32.0°±12.0°	0.72	No Order	No Order
SS-GrBP5	25.5°±5.5°	1.20	36.0°±1.0°	0.34